http://dx.doi.org/10.7566/JPSJ.82.124714

Linearized Augmented Plane-Wave and Muffin-Tin Orbital Method with the PBE Exchange–Correlation: Applied to Molecules from H_2 through Kr_2

Takao KOTANI[1] and Hiori KINO[2]

[1]*Department of Applied Mathematics and Physics, Tottori University, Tottori 680-8552, Japan*
[2]*National Institute for Materials Science, Tsukuba, Ibaraki 305-0047, Japan*

(Received June 11, 2013; accepted September 18, 2013; published online November 18, 2013)

We show that we can efficiently calculate the atomization energies of homogeneous diatomic molecules from H_2 through Kr_2 within the convergence of chemical accuracy ($\lesssim$1 kcal/mol) using an all-electron full-potential linearized mixed-basis method which has recently been proposed by one of the authors, in the density functional calculations using the PBE exchange correlation functional. The method is unique compared with other mixed-basis methods in that we simultaneously use two kinds of augmented waves as bases in the framework of the linearized method: the augmented plane waves (APWs) and the muffin-tin orbitals (MTOs). These two bases are responsible for the efficient representation of extended nature and localized nature of wavefunctions. We use a new simple prescription to determine parameters of MTOs. Owing to the inclusion of the MTOs, we can attain the convergence of chemical accuracy only with a very small number of APWs (cutoff energy of APWs is typically $\sim$4 Ry).

KEYWORDS: density functional, PBE, LAPW, LMTO, PAW, mixed basis, atom, dimer, supercell

1. Introduction

Today the first-principles electronic structure calculations are applied to wide range of problems in material science. To perform such calculations, a key is an one-body problem solver for some mean-field theories, a common one being the density functional theory (DFT) with the exchange–correlation energy in the local density approximation (LDA) or generalized gradient approximation (GGA). Even in other mean-field theories such as the quasiparticle self-consistent *GW* (QSGW) method[1)] that go beyond the DFT, the one-body problem solver is a key to obtaining numerically accurate results with minimum computational effort.[2,3)]

Except for the KKR method, commonly used one-body problem solvers in the physics community may be classified into the pseudopotential method, the projector augmented wave (PAW) method, and the full-potential linearized augmented wave methods such as the linearized augmented plane wave method (LAPW) and the linearized muffin-tin orbital method (LMTO).[3–8)] In these methods, we represent wavefunctions as superpositions of basis functions. The pseudopotential method is limited in accuracy due to the transferability problem; its results can be dependent on the quality of the pseudopotentials. In contrast, the PAW method given by Blöchl[4)] has sufficient accuracy in principle, comparable to the accuracy of the LAPW methods. The PAW method implemented in the Vienna ab-initio package (VASP)[5)] is widely used now. Its reliability depends on the quality of the projectors; the VASP generally uses only two projector functions per angular momentum $L \equiv (l, m)$ although these two are carefully chosen. The LAPW method is supposed to be more reliable in the sense that it does not depend on pseudopotentials nor such projectors, thus, there is no transferability problem in principle.

The general theory of the linearized augmented wave methods was proposed by Andersen in 1975,[9)] followed by many improvements and extensions.[3,4,6–8,10–13)] In the linearized augmented wave methods, wavefunctions are represented as superpositions of the augmented waves. The LAPW uses the augmented plane waves (APWs) made of plane waves (PWs) as envelope functions. In the following, we use the term APW to mean a basis used in the linearized method, not the original Slater's APW method. The LMTO uses muffin-tin orbitals (MTOs) made of the atom-centered smooth Hankel functions (smHankel functions)[8)] as envelope functions. We give a short explanation of the smHankel functions at the beginning of Sect. 2. Owing to the augmentation procedure, these envelope functions are for describing only interstitial parts of wavefunctions. Corresponding to these envelope functions, the APWs fit to the extended nature of wavefunctions; in contrast, the MTOs fit to their localized nature. In this sense, the APWs and MTOs have opposite natures.

This fact indicates the shortcomings of the above two methods. The LAPW requires many APWs in order to represent sharp structures of wavefunctions just outside the muffin tins (MTs). For example, 3*d* orbitals of transition metals and 2*p* orbitals of 2nd-row atoms are typical cases. In contrast, the LMTO has problems for representing the extended nature of wavefunctions. For example, we sometimes need to place empty spheres between atoms, however, it becomes very difficult to describe systems with huge vacuum regions such as slab models of surfaces. Furthermore, it is not easy to enlarge a basis set systematically in order to check for numerical convergence. This is a common problem in methods with localized bases, such as the *Gaussian* in the quantum chemistry.

To overcome these shortcomings, Kotani and van Schilfgaarde introduced a new method. We named it the linearized augmented plane wave and muffin-tin orbital method (the PMT method).[14)] This is an all-electron full-potential mixed basis method using APWs and MTOs simultaneously. Within our knowledge, there are no other full-potential methods that use different kinds of augmented waves simultaneously. We can expand wavefunctions efficiently in both kinds of bases together. The PMT method

is based on the formulation given by Soler and Williams[10] where the high angular momentum parts of the APWs and MTOs within MTs are taken into account; this theory is also used as a basis of the PAW method.

In this paper, we show the results obtained using the PMT method applied to homonuclear diatomic molecules from Hydrogen through Krypton in a supercell. We use the Perdew–Burke–Ernzerhof (PBE) exchange–correlation functional[15] implemented in the manner given by White and Bird.[16] Then we see that the PMT method shows good convergence for atomization energies within $\lesssim$1 kcal/mol with extremely low energy cutoff on the APW bases ($\sim$4 Ry) because MTOs are used together. Note that diatomic molecules are difficult systems to treat by the linearized augmented wave methods because we need to use rather smaller MT radii than those used in solids.

A key point in this paper is the new simple prescription for setting parameters of MTOs without atom-specific optimizations given in Sect. 2. In fact, the most serious obstacle for the wide use of the full-potential LMTO is the difficulty in setting the parameters.[8] Note that this difficulty is common in methods utilizing a localized basis set. For example, in *Gaussian*, people spend much effort in preparing basis sets. Our results in this paper demonstrate not only the efficiency or accuracy of the PMT method, but also its robustness, that is, the PMT method can be essentially free of such difficulty in "tuning parameters of localized basis", owing to the inclusion of the APWs.

We have already shown how the PMT method works for solids;[14] even the full-potential LMTO without APWs can work well for solids.[1,8] Considering these facts, we expect the PMT method to be promising to in describing wide range of cases from molecules through solids on equal footing in the full potential scheme. After the explanation of the improved version of the PMT method in Sect. 2, we show the results from H_2 through Kr_2 in Sect. 3.

2. Method

First, let us explain the smHankel functions used as the envelope functions of MTOs. The smHankel functions are first introduced by Methfessel.[3,8,17] The spherical smHankel function $h_0(\mathbf{r})$, where the subscript 0 means $L \equiv (l,m) = (0,0)$, is defined by the Helmholtz equation with a gaussian source term $g_0(\mathbf{r}) = C\exp(-r^2/R_{\mathrm{SM}}^2)$ instead of δ-function [see Eq. (5) in Ref. 8];

$$(\nabla^2 + \epsilon)h_0(\mathbf{r}) = -4\pi g_0(\mathbf{r}), \tag{1}$$

where $C = 1/(\sqrt{\pi}R_{\mathrm{SM}})^3$ is a normalization constant. $\epsilon = -\kappa^2$ denotes a negative energy to specify the asymptotic damping behavior of $h_0(\mathbf{r})$. In the limit $R_{\mathrm{SM}} \to 0$ where $g_0(\mathbf{r})$ becomes δ-function (as a point charge), $h_0(\mathbf{r})$ becomes the usual Hankel function $h_0(\mathbf{r}) = \exp(-\kappa r)/r$. Because the source term is smeared with the radius R_{SM}, we have no divergent behavior at $r = 0$; the smHankel function bends over at $\sim R_{\mathrm{SM}}$ (see Fig. 1 in Ref. 8). From $h_0(\mathbf{r})$, we can have $h_L(\mathbf{r}) \equiv \mathcal{Y}_L(-\nabla)h_0(\mathbf{r})$ for any L with the spherical polynomial $\mathcal{Y}_L(\mathbf{r}) = r^l Y_L(\hat{\mathbf{r}})$. $Y_L(\hat{\mathbf{r}})$ is the real spherical harmonics, where $\hat{\mathbf{r}}$ is the normalized $\mathbf{r}$. $\mathcal{Y}_L(-\nabla)$ means to substitute $\mathbf{r}$ in $\mathcal{Y}_L(\mathbf{r})$ with $-\nabla$ (see Ref. 17 for details). Note that $h_L(\mathbf{r})$ is specified with a pair of parameters $(\epsilon, R_{\mathrm{SM}})$ through $h_0(\mathbf{r})$ defined in Eq. (1).

Table I. For each element (atomic species), we use the MTOs and LOs specified in this Table. For example, "He–B" means from Helium through Boron. $\epsilon = -\kappa^2$ (Ry) is the damping factor of the smooth Hankel functions.[8,17] We use two L-independent ϵ's, written as $\epsilon_a^{(1)}$ and $\epsilon_a^{(2)}$. See text.

	LO	Valence	$\epsilon_a^{(1)}$	$\epsilon_a^{(2)}$
H		1*s*2*p*3*d*4*f*	−0.1	−2
He–B	1*s*	2*s*2*p*3*d*4*f*	−0.1	−2
C–F		2*s*2*p*3*d*4*f*	−1	−2
Ne–Al	2*s*2*p*	3*s*3*p*3*d*4*f*	−0.1	−2
Si–Cl		3*s*3*p*3*d*4*f*	−1	−2
Ar–Mn	3*s*3*p*	4*s*4*p*3*d*4*f*	−0.1	−2
Fe–Ni	3*s*3*p*3*d*	4*s*4*p*4*d*4*f*	−0.1	−2
Cu–Ga	3*d*	4*s*4*p*4*d*4*f*	−0.1	−2
Ge–As	3*d*	4*s*4*p*4*d*4*f*	−1	−2
Se–Br		4*s*4*p*4*d*4*f*	−1	−2
Kr	4*s*4*p*	5*s*5*p*4*d*4*f*	−0.1	−2

In the following, we explain the PMT method briefly,[14] together with a new simple prescription for setting the parameters of MTOs to specify them.

In the PMT method, the all-electron density is given as a superposition of the core densities and valence electron density. The core density for each atom is given in the frozen core approximation, that is, the core density for each atom is determined in advance with the calculation for the spherical atom. (Note that rather deep states are treated as valence electrons in this paper. See Table I.)

The valence electron density is calculated from the valence eigenfunctions, which are represented as linear combinations of three kinds of bases as follows:

- APWs. They are specified by $\mathbf{q} + \mathbf{G}$. The cutoff energy $E_{\mathrm{MAX}}^{\mathrm{APW}}$ is given as $\frac{\hbar^2|\mathbf{q}+\mathbf{G}|^2}{2m} < E_{\mathrm{MAX}}^{\mathrm{APW}}$. The corresponding number of the APW bases is denoted by N_{APW}.
- MTOs. The atom-centered smHankel functions are used as their envelope functions.
- Local orbitals (LOs).[18] These are restricted within MTs. The envelope functions of LOs are zero everywhere.

MTOs and LOs are atom-centered localized orbitals, for which we take the Bloch sum for the wave vector $\mathbf{q}$ to recover translational symmetry. We apply the augmentation procedure to both the MTOs and the APWs. For the augmentation, we need two radial functions within MTs for each al [a is the index of MT and l is l of $L = (l,m)$]; they are often called ϕ_{al} and $\dot{\phi}_{al}$, which are the two solutions of the radial Schrodinger equations solved at energies around the center of gravity of the partial density of states for occupied states. For the construction of the LOs, we make linear combinations of the semi-core radial functions with ϕ_{al} and $\dot{\phi}_{al}$ such that the value and slope of the LOs at the MT boundaries are zero.[18]

Table I shows the MTOs and LOs used for each element (atomic species). We use two MTO bases for each aL for $0 \le l \le 3$ for all kinds of atoms treated here. Thus, we have $2 \times (\sum_{l\le 3}(2l+1)^2) = 32$ MTOs per atom. The indexes of the principle quantum number and angular momentum of MTOs for valence electrons are shown in the valence column in Table I. For example, 3*s*3*p*3*d*4*f* from Ne through Al means that we use the MTOs corresponding to these

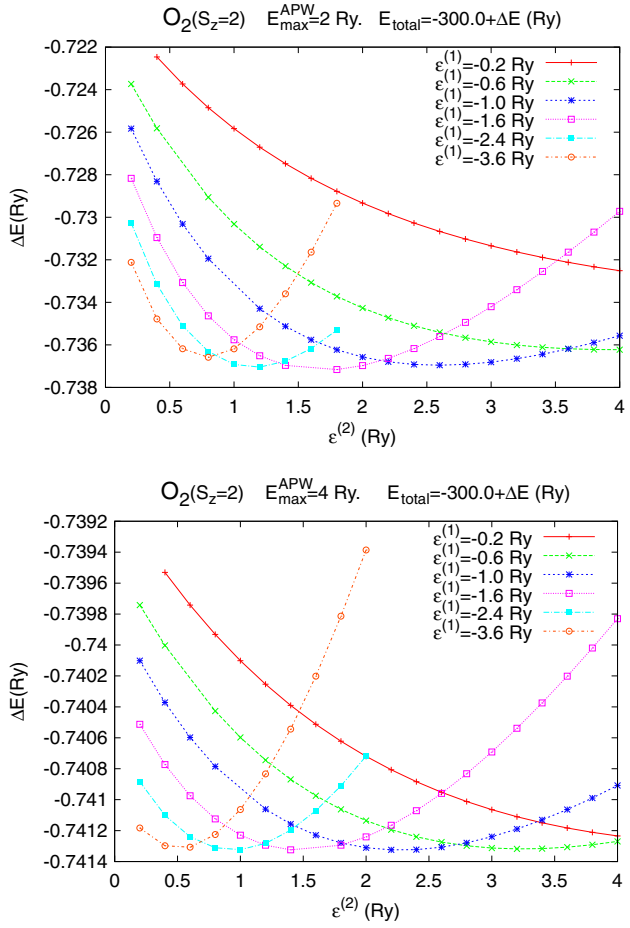

Fig. 1. (Color online) Dependence of the total energy for $O_2(S_z = 2)$ on $\epsilon_a^{(1)}, \epsilon_a^{(2)}$ (the subscript for specifying atom a, is omitted in the figures. The top panel is for $E_{\rm MAX}^{\rm APW} = 2\,{\rm Ry}$, the bottom panel is for $E_{\rm MAX}^{\rm APW} = 4\,{\rm Ry}$. We use a supercell of $10\,{\rm \AA}^3$ and the MT radius $R_a = 0.610\,{\rm \AA}$. The atomic distance is $1.220\,{\rm \AA}$. Note that the energy scale of the bottom panel is approximately ten times smaller than that of the top panel. The dependence of the total energy on $\epsilon_a^{(1)}, \epsilon_a^{(2)}$ becomes much smaller at $E_{\rm MAX}^{\rm APW} = 4\,{\rm Ry}$ than at $E_{\rm MAX}^{\rm APW} = 2\,{\rm Ry}$.

quantum numbers. Because we use two MTO bases for each aL, we have to specify two smHankel functions, that is, we have to specify two pairs of $(\epsilon, R_{\rm SM})$ for all kinds of atoms. The two ϵ parameters are independent of L and are tabulated as $\epsilon_a^{(1)}, \epsilon_a^{(2)}$ in Table I. As Table I shows, we utilize a very simple setting: $\epsilon_a^{(1)}, \epsilon_a^{(2)} = -0.1, -2\,{\rm Ry}$ for the left-hand-side elements in the periodic table; $\epsilon_a^{(1)}, \epsilon_a^{(2)} = -1, -2\,{\rm Ry}$ for the right-hand-side elements. These $\epsilon_a^{(1)}, \epsilon_a^{(2)}$ are semi-optimum values as we will explain in Fig. 1 as follows. On the choice of $R_{\rm SM}$, we use $R_{\rm SM} = R_a/2$ for all MTOs (thus not tabulated here), where R_a is the muffin-tin radius of the atom a. The condition $R_{\rm SM} = R_a/2$ is chosen through preliminary test calculations, where we calculated the total energies for different ratios of $R_a/R_{\rm SM}$. Generally (not always), we see the tendency that smaller $R_{\rm SM}$ gives lower total energy. Because $R_{\rm SM} = R_a/2$ is small enough that smHankel functions behave almost like usual Hankel functions outside MTs, MTOs made of such smHankel functions are almost similar to those made of usual Hankel functions (the total energy hardly depends on $R_{\rm SM}$, as long as it is small enough). In other words, we have decided not to use the degree of freedom of $R_{\rm SM}$ to chose the envelope functions of MTOs. Thus the only reason of using smHankel functions instead of usual Hankel functions is to obtain non-divergent smooth part of the electron density; the smooth part of the electron density (made of the envelope functions) is required in the formulation by Soler and Williams.[10] Because the density should be expanded in plane waves, it is not efficient to use very small $R_{\rm SM}$. Nonetheless the results shown in Sect. 3 are a justification that our prescription works well, although we can not exclude the fact that there are better choices of $R_{\rm SM}$.

The above prescription giving MTOs is very different from that in the usual LMTO method,[8] where we are required to optimize the parameters of MTOs carefully because of the limited number of bases in the LMTO method. The optimization of $R_{\rm SM}$ is based on the idea to mimic the bending of eigenfunctions just outside MTs with the choice of $R_{\rm SM}$. However, such optimization inevitably involves the choice of $\epsilon_a^{(1)}, \epsilon_a^{(2)}$; it is too complicated as shown in figures of Ref. 8. This difficulty is a serious problem in the LMTO methods. The PMT method with the above prescription is free of this problem.

We use the LOs for *al* channels specified in Table I. For example, from Ne through Al, $2s$ and $2p$ are treated as LOs, resulting in a total number of 32+4 atom-centered bases. From Fe through Ni, we use 32+16 atom-centered bases. We use these LOs to describe the spilling out of the corresponding semi-core states outside MTs. In addition, employing such LOs can stabilize calculations because it ensures the orthogonality of the valence eigenfunctions with the semi-core states treated as LOs. In some atoms, it is better to treat even rather deep states as LOs because of the small MT radius R_a due to the short atomic distances of molecules.

In summary, we specify a new simple prescription for setting up a basis set. The indexes of the bases are given as $\{\mathbf{qG}, \mathbf{q}aLn\}$, $\mathbf{G}$ for the APWs, and aLn for the MTOs and LOs. Here, n is for specifying the MTOs and LOs. Orbitals with lower principle quantum numbers than those of the MTOs and LOs are treated as frozen cores.

Let us explain why we chose values of $\epsilon_a^{(1)}, \epsilon_a^{(2)}$ for elements in Table I. To determine them, we made plots on how the total energy depends on $\epsilon_a^{(1)}, \epsilon_a^{(2)}$ in the supercell calculations of atoms and molecules. For example, Fig. 1 is for O_2. In this case, there are parameters that give the minimum total energy. For example, $(\epsilon_a^{(1)}, \epsilon_a^{(2)}) \sim (-1.6, -1.8)\,{\rm Ry}$ gives the energy minimum at $E_{\rm MAX}^{\rm APW} = 2\,{\rm Ry}$ (top panel). However, broader parameter sets can give almost similar lowest energies at $E_{\rm MAX}^{\rm APW} = 4\,{\rm Ry}$ (bottom panel); the sets of $(\epsilon_a^{(1)}, \epsilon_a^{(2)}) \sim (-1.0, -2.2)\,{\rm Ry}$, $\sim(-1.6, -1.4)\,{\rm Ry}$, and so on, give almost similar lowest energy. More importantly, we see the fact that the energy dependence on $(\epsilon_a^{(1)}, \epsilon_a^{(2)})$ becomes much smaller at $E_{\rm MAX}^{\rm APW} = 4\,{\rm Ry}$ than at $E_{\rm MAX}^{\rm APW} = 2\,{\rm Ry}$; note the energy scale of the y-axis. This means that the tuning of $(\epsilon_a^{(1)}, \epsilon_a^{(2)})$ is less meaningful when we use a larger $E_{\rm MAX}^{\rm APW}$. Other atoms and molecules show essentially similar dependence on $E_{\rm MAX}^{\rm APW}$. Because we can perform a convergence check simply by changing the number of APWs, we do not need to stick to the optimization of $\epsilon_a^{(1)}, \epsilon_a^{(2)}$ strictly. Thus it is sufficient to make a rough optimization for the set of $\epsilon_a^{(1)}, \epsilon_a^{(2)}$. From similar plots for the other atoms, we have decided to use the simple setting of $\epsilon_a^{(1)}, \epsilon_a^{(2)}$ shown in Table I.

3. Results and Discussions

From Hydrogen through Krypton, we calculated ferro-magnetic (or non-magnetic) ground states for atoms and homonuclear diatomic molecules for the spin-polarized DFT calculations in the PBE.[15] We also calculated spin-excited states in some cases.

Following Ref. 19, we use a large orthogonal supercell $13.5 \times 15 \times 16.5\,\text{Å}^3$ to avoid interactions between molecules in periodic cells. We use Γ point only in the Brillouin zone summation. A diatomic molecule is placed along the $(1,1,1)$ direction in the Cartesian coordinates. This only allows inversion symmetry; this helps us to find symmetry-broken ground states. Atoms are also calculated with similar supercells. The atomization energy for a molecule is calculated with a procedure subtracting twice of the total energy of an atom from the total energy of a molecule as Eq. (46) in Ref. 19. We mainly show the results in the scalar relativistic (SR) approximations; the convergence checks shown here are for the results. We also performed calculations in the non-relativistic (NR) approximation. To check our calculations, we performed calculations with *Gaussian03* with the condition PBE/6-311+G(d,p),scf(tight) by ourselves. All the calculations are under the constraint of the spin moment S_z. For the real-space mesh for describing the smooth part of electron densities and one-body potentials, we use the cutoff $E_{\text{MAX}}^{\text{rmesh}} = 144\,\text{Ry}$.

In the SR approximations, all the ground state energies for atoms and diatomic molecules are obtained with integer occupancy (zero or unity) for all one-electron states. In the case of NR approximation, this is also true except for two cases of atoms Ni($2S_z = 2$) and V($2S_z = 5$), where we have degenerated HOMO states (thus converged with fractional occupancies). We have also observed such fractional occupancies for ferro-magnetic excited states, e.g., O($S_z = 0$) and Ni_2($S_z = 0$) (not shown in this paper). Even among other cases with integer occupancy, cases in which the LUMO–HOMO gaps are very small exist, probably because the gaps are caused by the anisotropy of our supercell. This is not an easy problem which is related to the localization/delocalization error.[20] Thus, we do not treat this problem here; we just show the results of the ground states (and spin-excited states) obtained by our procedure.

In Fig. 2, we plot the ground-state total energies of an atom in the supercell as a function of $E_{\text{MAX}}^{\text{APW}}$ to check for convergence. We show three typical cases, N($2S_z = 3$), O($2S_z = 2$), and Fe($2S_z = 4$), using three different R_a for each atom. The maximum R_a is chosen such that they are almost one half of the equilibrium atomic distances. Corresponding to different $E_{\text{MAX}}^{\text{APW}}$, N_{APW} range from 1081 through 8611 (see figure caption). In the case of the main group elements such as N($2S_z = 3$) and O($2S_z = 2$), the change in E_e is only 1–2 mRy even when we change the number of bases from $E_{\text{MAX}}^{\text{APW}} = 4\,\text{Ry}$ to $E_{\text{MAX}}^{\text{APW}} = 8\,\text{Ry}$. In contrast, we see a slower convergence for transition metals such as Fe($2S_z = 4$) than for the main group elements. This difference can be due to the difference of sharpness of the eigenfunctions just outside MTs. We can state that the number of MTOs are not large enough to weaken the $E_{\text{MAX}}^{\text{APW}}$ dependence. However, we can obtain the converged values

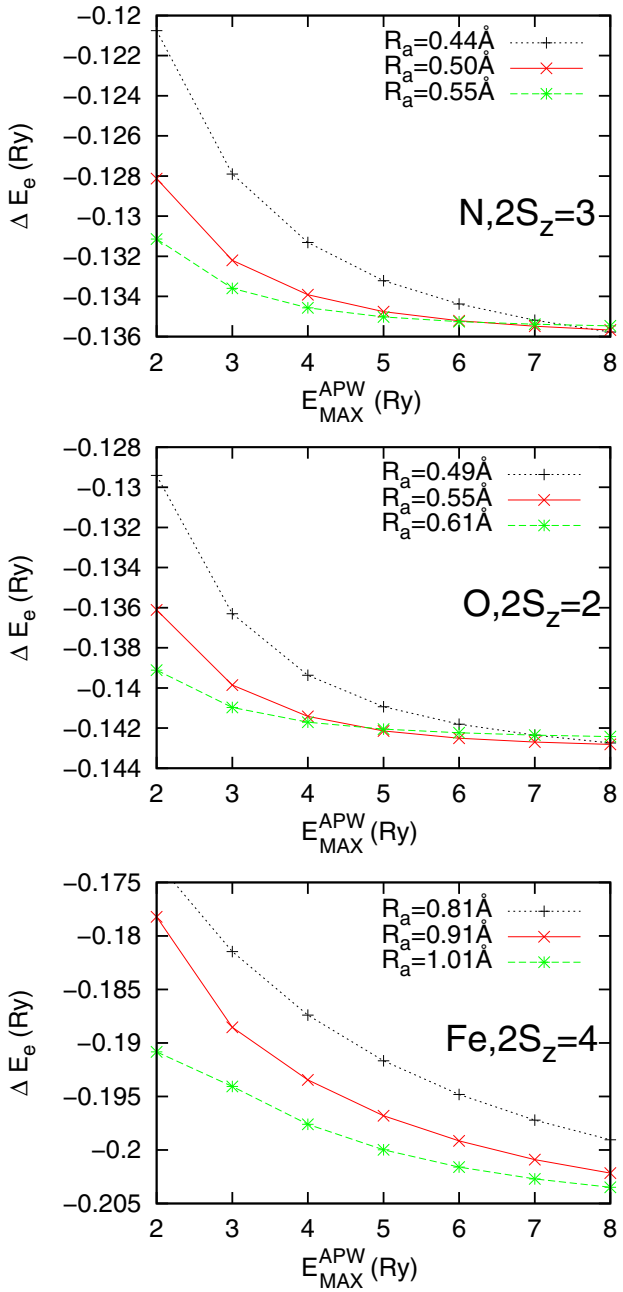

Fig. 2. (Color online) Total energy of an atom in a supercell as a function of $E_{\text{MAX}}^{\text{APW}}$ to check for convergence on $E_{\text{MAX}}^{\text{APW}}$. We just show the fractional parts of energies ΔE_e (in Ry) for N($2S_z = 3$), O($2S_z = 2$), and Fe($2S_z = 4$). For each atom, we use three MT radii. The number of APWs, N_{APW}, used are 1081, 1973, 3025, 4245, 5573, 7025, and 8611 for $E_{\text{MAX}}^{\text{APW}} = 2, 3, \ldots,$ 8 Ry, respectively.

of physical properties such as atomization energies with relatively low $E_{\text{MAX}}^{\text{APW}}$ even for Fe($2S_z = 4$) as shown in the following. On the R_a dependence, we see that larger R_a gives lower energies for small $E_{\text{MAX}}^{\text{APW}}$ because of the advantage of more effective augmentation. However, the advantage using large R_a disappears when we use large $E_{\text{MAX}}^{\text{APW}}$. In fact, a detailed look at the N($2S_z = 3$) and O($2S_z = 2$) panels near $E_{\text{MAX}}^{\text{APW}} = 8\,\text{Ry}$ shows that smaller R_a can reach slightly lower energies for larger $E_{\text{MAX}}^{\text{APW}}$. This indicates that the error of augmentation overrides the error in the interstitial region when the number of APWs is large enough. Recall that eigenfunctions within MTs are spanned

Table II. Quantities at equilibrium positions; atomic distance r_e (Å), atomization energy D_e (kcal/mol), and harmonic vibrational frequency ω_e (cm^{-1}) are tabulated for a number of molecules as functions of E_{MAX}^{APW} to check for convergence on E_{MAX}^{APW}. The MT radius R_a (Å) used is shown. We also show only D_e (kcal/mol) in other cases in Table III. 1 eV = 1/13.605 Ry = 23.06 kcal/mol.

E_{MAX}^{APW}	$He_2, 2S_z = 0$ $R_a = 1.05$			$Na_2, 2S_z = 0$ $R_a = 1.08$			$Si_2, 2S_z = 2$ $R_a = 1.04$			$Se_2, 2S_z = 2$ $R_a = 0.99$			$Zn_2, 2S_z = 2$ $R_a = 1.28$		
	r_e	D_e	ω_e	r_e	D_e	ω_e	r_e	D_e	ω_e	r_e	D_e	ω_e	r_e	D_e	ω_e
2	2.756	.0748	66.81	3.086	17.68	155.8	2.286	81.24	484.	2.195	93.85	377.	3.159	1.57	49.2
3	2.757	.0745	66.69	3.087	17.67	156.3	2.286	81.18	483.	2.195	93.85	377.	3.159	1.56	49.1
4	2.757	.0740	66.46	3.086	17.65	156.3	2.286	81.17	483.	2.194	93.87	378.	3.158	1.57	49.1

E_{MAX}^{APW}	$C_2, 2S_z = 2$ $R_a = 0.59$			$O_2, 2S_z = 2$ $R_a = 0.55$			$V_2, 2S_z = 2$ $R_a = 0.78$			$Cr_2, 2S_z = 0$ $R_a = 0.72$			$Fe_2, S_z = 6$ $R_a = 0.91$		
	r_e	D_e	ω_e	r_e	D_e	ω_e	r_e	D_e	ω_e	r_e	D_e	ω_e	r_e	D_e	ω_e
2	1.312	160.01	1648.	1.218	143.86	1567.	1.739	81.37	679.	1.589	35.08	819.	1.984	57.83	418.
3	1.312	159.69	1648.	1.218	143.74	1565.	1.741	79.99	680.	1.590	33.70	815.	1.987	57.18	415.
4	1.312	159.66	1648.	1.218	143.73	1565.	1.742	79.22	681.	1.591	32.83	813.	1.989	57.01	413.
5	1.312	159.72	1648.	1.218	143.76	1565.	1.743	78.78	681.	1.591	32.29	811.	1.991	56.87	412.
6	1.312	159.81	1648.	1.218	143.78	1568.	1.744	78.56	681.	1.592	31.99	808.	1.992	56.84	411.
7	1.312	159.92	1648.	1.218	143.79	1568.	1.744	78.44	681.	1.593	31.85	807.	1.992	56.85	411.

by a few partial waves for each L, therefore, it is reasonable that we can reach lower energies with smaller R_a as long as we use many bases in the interstitial region.

In Table II, we show the atomic equilibrium distance r_e, the atomization energy D_e and harmonic vibrational frequency ω_e as functions of E_{MAX}^{APW} to check for convergence on E_{MAX}^{APW}. We use kcal/mol for D_e in all Tables: 1 eV = 1/13.605 Ry = 23.06 kcal/mol. In addition, we show only D_e in other typical cases in Table III, where the results for O_2 and Fe_2 obtained with the use of different R_a are also included. From these Tables, we can see that the physical properties converge fast enough on E_{MAX}^{APW}; we may claim that the convergence of D_e is approximately at ~1 kcal/mol level (chemical accuracy) or even higher. For example, $Fe_2(S_z = 6)$ with $R_a = 0.91$ Å in Table II shows that D_e changes from 57.18 kcal/mol (at $E_{MAX}^{APW} = 3$ Ry) to 56.85 kcal/mol (at $E_{MAX}^{APW} = 7$ Ry); the difference is only 0.33 kcal/mol. Considering the slow convergence of Fe shown in Fig. 2, this indicates that error cancellation works well in the PMT method between the total energy of dimers and that of two atoms. That is, the error due to the cutoff of E_{MAX}^{APW} has an atomic nature and is included in the same manner in two calculations for an atom and for a dimer. Even with low E_{MAX}^{APW}, the important bonding part is described well. It is not easy to use E_{MAX}^{APW} larger than ~7 Ry together with the MTOs used here, because the overcompleteness of the basis set tends to destabilize our calculations. However, the results with E_{MAX}^{APW} up to 7 Ry show satisfactory stability (or convergence) on D_e. In the other transition metal dimers, we see a similar or slightly poorer convergence behavior. For example, we see slightly slower convergence in the case of V_2. We can roughly see the size or convergence error of D_e from Tables II and III. Even considering cases such as V_2, we can claim that $E_{MAX}^{APW} = 4$ Ry is almost large enough to attain an error of ~1 kcal/mol for D_e.

Let us examine the stability of our results on the MT size R_a, e.g., see the case of $Fe_2(S_z = 6)$. The best estimate of $D_e = 56.85$ kcal/mol at $E_{MAX}^{APW} = 7$ Ry in Table II changes to 56.79 kcal/mol and to 57.06 kcal/mol for ±10% changes in R_a as shown in Table III. We can state that the stability on R_a is satisfactory enough. Because these values converge well on E_{MAX}^{APW}, we can identify the difference to be due to the augmentation error resulting from the fact that only a few partial waves are used for each L within MTs.

In Table IV, we show our final results for all the homonuclear dimers treated here. Our main results obtained in the PMT method are compared with those in *Gaussian03* labeled as GTO, and those in VASP.[19] In addition to the results obtained in PMT in the SR approximation, we show those in the NR approximation, labeled as PMT(NR). For example, let us look in the section of "$O_2, 2S_z = 2$". D_e = 143.8 kcal/mol for PMT is consistent with 143.3 kcal/mol for VASP. This is also true in other cases. The GTO value of 139.8 kcal/mol and the PMT(NR) value of 144.0 kcal/mol show a little discrepancy, although both methods are in the NR approximation. This is also the case for other elements N_2, O_2, F_2, P_2, S_2, and Cl_2. However, it is known that this error for the right-hand-side elements in the periodic table is due to the inadequate polarized d bases in the GTO basis set (the GTO calculations with a larger basis set show better agreement with those given in VASP[19]). Except these cases, D_e in GTO are in good agreement with those in PMT(NR) for the main group elements (within ~1 kcal/mol difference). For transition-metal elements, we think that the results are consistent enough although we see a little differences in cases. For example, D_e = 59.4 kcal/mol in PMT(NR) for "$Ni_2, 2S_z = 2$" is a little different from 63.2 kcal/mol in GTO, although the PMT(NR) value converges as well as the SR value shown in Table III.

We can see a tendency that the SR approximation gives smaller r_e than the NR approximation for heavy elements. For example, in the case of "$Cu_2, 2S_z = 0$", the difference in r_e between PMT and PMT(NR) is 0.03 Å. In addition, there is a non-negligible difference in D_e, i.e., 4.2 kcal/mol.

Generally speaking, our results indicate that the missing part of the Hilbert space spanned by a localized basis set can be systematically complemented well by low-energy

Table III. Similar to Table II, but only the atomization energies D_e (kcal/mol) are shown. Results for O_2 and Fe_2, $2S_z = 6$ use different R_a from those in Table II are shown. A negative sign of Mn_2, $2S_z = 2$ means that the atomization energy is positive.

$E_{\mathrm{MAX}}^{\mathrm{APW}}$	$B_2, 2S_z = 4$ $R_a = 0.69$ D_e	$N_2, 2S_z = 0$ $R_a = 0.44$ D_e	$N_2, 2S_z = 0$ $R_a = 0.50$ D_e	$N_2, 2S_z = 0$ $R_a = 0.55$ D_e	$O_2, 2S_z = 2$ $R_a = 0.49$ D_e	$O_2, 2S_z = 2$ $R_a = 0.61$ D_e	$F_2, 2S_z = 0$ $R_a = 0.64$ D_e	$P_2, 2S_z = 0$ $R_a = 0.86$ D_e	$S_2, 2S_z = 2$ $R_a = 0.87$ D_e	$Cl_2, 2S_z = 0$ $R_a = 0.92$ D_e
2	79.67	246.41	244.22	243.60	144.82	143.87	53.31	121.65	114.97	65.44
3	79.46	245.41	243.95	243.47	144.36	143.71	53.23	121.40	115.01	65.50
4	79.41	244.91	243.88	243.47	144.20	143.69	53.20	121.35	115.06	65.52
5	79.38	244.59	243.85	243.48	144.11	143.69	53.19	121.36	115.09	65.51
6	79.37	244.37	243.81	243.47	144.04	143.69	53.18	121.37	115.12	65.51
7	79.37	244.20	243.78	243.46	143.98	143.69	53.16	121.38	115.15	65.53

$E_{\mathrm{MAX}}^{\mathrm{APW}}$	$Sc_2, 2S_z = 2$ $R_a = 1.18$ D_e	$Sc_2, 2S_z = 4$ $R_a = 1.18$ D_e	$Ti_2, 2S_z = 2$ $R_a = 0.85$ D_e	$V_2, 2S_z = 0$ $R_a = 0.78$ D_e	$Cr_2, 2S_z = 2$ $R_a = 0.72$ D_e	$Cr_2, 2S_z = 4$ $R_a = 0.72$ D_e	$Mn_2, 2S_z = 2$ $R_a = 0.74$ D_e	$Mn_2, 2S_z = 10$ $R_a = 0.74$ D_e
2	33.46	37.07	70.96	70.94	10.85	0.61	−6.38	18.14
3	33.37	36.98	69.84	69.57	9.67	−0.47	−6.08	19.32
4	33.37	36.98	69.30	68.81	8.95	−1.11	−5.90	20.02
5	33.39	37.00	69.05	68.38	8.54	−1.44	−5.81	20.39
6	33.41	37.01	68.95	68.17	8.34	−1.57	−5.72	20.60
7	33.46	37.05	68.94	68.06	8.27	−1.57	−5.59	20.71

$E_{\mathrm{MAX}}^{\mathrm{APW}}$	$Fe_2, 2S_z = 6$ $R_a = 0.80$ D_e	$Fe_2, 2S_z = 6$ $R_a = 1.01$ D_e	$Fe_2, 2S_z = 8$ $R_a = 0.80$ D_e	$Fe_2, 2S_z = 8$ $R_a = 0.91$ D_e	$Fe_2, 2S_z = 8$ $R_a = 1.01$ D_e	$Co_2, 2S_z = 4$ $R_a = 0.96$ D_e	$Ni_2, 2S_z = 2$ $R_a = 0.89$ D_e	$Cu_2, 2S_z = 0$ $R_a = 1.01$ D_e
2	57.79	58.34	50.51	50.42	50.99	62.92	66.13	53.22
3	57.11	57.48	49.90	49.78	50.08	62.09	65.47	52.64
4	56.80	57.29	49.65	49.62	49.90	61.66	65.19	52.39
5	56.71	57.15	49.59	49.52	49.77	61.41	65.06	52.30
6	56.72	57.09	49.60	49.51	49.71	61.28	65.02	52.29
7	56.79	57.06	49.65	49.51	49.69	61.29	65.04	52.30

APWs. Note that $E_{\mathrm{MAX}}^{\mathrm{APW}} = \frac{\hbar^2|\mathbf{q}+\mathbf{G}|^2}{2m} = 4\,\mathrm{Ry}$, which is required to attain chemical accuracy, gives $|\mathbf{q}+\mathbf{G}| \approx 2\pi/(1.6\,\text{Å})$. This denominator roughly corresponds to the atomic distances of dimers. This indicates that good convergence of D_e with low $E_{\mathrm{MAX}}^{\mathrm{APW}}$ achieved because low energy APWs improve description of atomic bonds efficiently. The APWs are no-center bases, suitable for describing atomic bonds without specifying the center of atomic bonds.

In order to evaluate the advantages of the PMT method, let us estimate the number of bases required for a large supercell calculation. For example, consider one hundred atoms in a supercell of $15 \times 15 \times 15\,\text{Å}^3$. In this case, we estimate required number of bases is $\sim 3000 + 30 \times 100$, where 3000 are from the APWs of $E_{\mathrm{MAX}}^{\mathrm{APW}} = 4\,\mathrm{Ry}$ and 30×100 are from MTOs (here, we assume that the number of MTOs per atom is ∼30). Because $N_{\mathrm{APW}} \propto (E_{\mathrm{MAX}}^{\mathrm{APW}})^{3/2}$ and the eigenvalue problem requires computational effort $\propto N^3$, the reduction in N_{APW} is important to reduce computational effort. From our experiences, the cutoff energy $E_{\mathrm{MAX}}^{\mathrm{APW}} \sim 4\,\mathrm{Ry}$ is also good enough to describe solids such as SiO_2 where we have large empty regions without empty spheres, as long as we use two or more MTOs per L. Therefore we expect that the PMT method can become a useful tool as a one-body problem solver that can treat both molecules and solids together on an equal footing in a much more inexpensive manner.

4. Summary

We have shown the results of DFT calculations in the PBE for homonuclear diatomic molecules from H_2 through Kr_2 using the recently developed PMT method. We give a new simple prescription for setting parameters to specify MTOs. Because of the prescription, we are not bothered with setting th parameters to specify MTOs. Thus we have performed supercell calculations for the molecules. We check for convergence by changing the cutoff energy $E_{\mathrm{MAX}}^{\mathrm{APW}}$, which determines the number of APWs. The PMT method can be accurate enough to attain the convergence of chemical accuracy (∼1 kcal) for the atomization energies D_e only with small numbers of APWs $E_{\mathrm{MAX}}^{\mathrm{APW}} \sim 4\,\mathrm{Ry}$, owing to the inclusion of MTOs. We show D_e, the atomic equilibrium distance r_e, and the harmonic vibrational frequency ω_e for the molecules in the scalar relativistic approximations and in non-relativistic calculations. The results show good agreement with those in the literature obtained using VASP. The agreement with those obtained using *Gaussian03* (performed by ourselves) also looks reasonable. In addition, we see systematic differences between the scalar relativistic and non-relativistic calculations. Because of the efficiency and accuracy of the PMT method with the new simple prescription for setting MTOs, we expect that the PMT method will be a useful one-body

Table IV. Our results for the homonuclear diatomic molecules, compared with those obtained by Gaussian and VASP. The used units are r_e (Å), D_e (kcal/mol), and ω_e (cm^{-1}). The PMT is in the scalar relativistic approximation, PMT(NR) is in the non-relativistic approximation. GTO means the calculations with *Gaussian03* with the basis set PBE/6-311+G(d,p),scf(tight). VASP denotes data cited from Ref. 19. As we noted in the text, the GTO calculations show some systematic error for the right-hand-side elements in the periodic table because of the basis set. Calculations are performed with $E_{MAX}^{APW} = 4\,Ry$ or $E_{MAX}^{APW} = 7\,Ry$ (when we use $E_{MAX}^{APW} = 7\,Ry$, $*$ is added to left column as "$B_2,2S_z = 2,*$").

		r_e	D_e	ω_e
$H_2,2S_z = 0$	PMT	0.749	104.7	4318.
	PMT(NR)	0.750	104.8	4311.
	GTO	0.752	104.6	4312.
$He_2,2S_z = 0$	PMT	2.757	0.074	66.5
	PMT(NR)	2.758	0.170	66.4
	GTO	2.656	0.098	87.5
$Li_2,2S_z = 0$	PMT	2.729	19.9	334.
	PMT(NR)	2.729	20.1	334.
	GTO	2.735	20.2	333.
	VASP		19.9	
$Be_2,2S_z = 0$	PMT	2.434	9.78	348.
	PMT(NR)	2.434	9.97	348.
	GTO	2.433	9.79	349.
$B_2,2S_z = 2,*$	PMT	1.618	77.0	1017.
	PMT(NR)	1.618	77.1	1018.
	GTO	1.621	76.5	1019.
$B_2,2S_z = 4,*$	PMT	1.529	79.4	1258.
	PMT(NR)	1.529	79.4	1257.
	GTO	1.532	79.0	1260.
$C_2,2S_z = 2,*$	PMT	1.312	159.9	1648.
	PMT(NR)	1.313	160.0	1646.
	GTO	1.317	157.3	1647.
$N_2,2S_z = 0,*$	PMT	1.102	243.8	2358.
	PMT(NR)	1.102	243.9	2361.
	GTO	1.107	239.4	2350.
	VASP		243.7	
$O_2,2S_z = 2,*$	PMT	1.218	143.8	1568.
	PMT(NR)	1.218	144.0	1569.
	GTO	1.220	139.8	1554.
	VASP		143.3	
$F_2,2S_z = 0,*$	PMT	1.414	53.2	997.
	PMT(NR)	1.413	53.2	998.
	GTO	1.430	47.5	930.
	VASP		52.6	
$Ne_2,2S_z = 0$	PMT	3.061	0.137	38.0
	PMT(NR)	3.062	0.425	38.0
	GTO	3.036	0.176	38.9
$Na_2,2S_z = 0$	PMT	3.086	17.7	156.4
	PMT(NR)	3.091	18.0	156.0
	GTO	3.090	17.8	155.5
	VASP		17.7	
$Mg_2,2S_z = 0$	PMT	3.512	3.16	99.9
	PMT(NR)	3.510	3.46	100.5
	GTO	3.503	3.26	101.4
$Al_2,2S_z = 2$ (two minima)	PMT	2.488	38.3	340.3
	PMT(NR)	2.489	38.8	340.9
	GTO	2.493	37.3	340.1
	PMT	2.756	37.4	256.5
	PMT(NR)	2.756	37.9	259.6
	GTO	2.783	36.7	279.7
$Si_2,2S_z = 2$	PMT	2.286	81.2	483.
	PMT(NR)	2.286	81.8	485.
	GTO	2.301	77.6	467.
	VASP		81.3	
$P_2,2S_z = 0,*$	PMT	1.904	121.4	783.
	PMT(NR)	1.905	121.6	784.
	GTO	1.913	115.7	773.
	VASP		121.5	
$S_2,2S_z = 2,*$	PMT	1.910	115.2	703.
	PMT(NR)	1.909	115.5	705.
	GTO	1.936	106.3	669.
	VASP		115.4	
$Cl_2,2S_z = 0,*$	PMT	2.007	65.5	538.
	PMT(NR)	2.006	65.7	540.
	GTO	2.053	57.0	501.
	VASP		65.8	
$Ar_2,2S_z = 0$	PMT	4.003	0.139	22.2
	PMT(NR)	4.006	0.335	22.2
	GTO	4.021	0.165	28.6
$K_2,2S_z = 0$	PMT	3.989	13.5	88.5
	PMT(NR)	4.004	13.7	88.1
	GTO	4.001	13.3	88.7
$Ca_2,2S_z = 0$	PMT	4.105	6.0	88.7
	PMT(NR)	4.094	6.6	90.7
	GTO	4.157	5.2	82.6
$Sc_2,2S_z = 2,*$	PMT	2.602	33.5	264.
	PMT(NR)	2.609	34.4	261.
	GTO	2.608	33.6	255.
$Sc_2,2S_z = 4,*$	PMT	2.617	37.1	251.
	PMT(NR)	2.617	38.0	250.
	GTO	2.626	37.7	242.
$Ti_2,2S_z = 2,*$	PMT	1.910	68.9	451.
	PMT(NR)	1.897	67.9	464.
	GTO	1.897	68.1	463.
$V_2,2S_z = 0,*$	PMT	1.741	68.1	654.
	PMT(NR)	1.739	65.9	685.
$V_2,2S_z = 2,*$	PMT	1.744	78.4	681.
	PMT(NR)	1.742	76.3	668.
	GTO	1.740	75.4	654.
$Cr_2,2S_z = 0,*$	PMT	1.593	31.9	807.
	PMT(NR)	1.591	28.3	812.
	GTO	1.595	26.2	808.
$Cr_2,2S_z = 2,*$	PMT	1.685	8.3	675.
	PMT(NR)	1.683	5.2	678.
$Cr_2,2S_z = 4,*$	PMT	1.792	−1.6	567.
	PMT(NR)	1.789	−4.3	566.

Continued on next page.

Continued.

		r_e	D_e	ω_e
$Mn_2, 2S_z = 2, *$	PMT	1.646	−5.6	674.
	PMT(NR)	1.644	−0.6	677.
	GTO	1.648	−1.8	667.
$Mn_2, 2S_z = 10, *$	PMT	2.588	20.7	211.
	PMT(NR)	2.608	25.2	207.
$Fe_2, 2S_z = 6, *$	PMT	1.993	56.8	398.
	PMT(NR)	1.994	58.4	386.
	GTO	2.012	56.9	397.
$Fe_2, 2S_z = 8, *$	PMT	2.129	49.5	334.
	PMT(NR)	2.157	48.0	267.
$Co_2, 2S_z = 4$	PMT	1.962	61.3	402.
	PMT(NR)	1.972	55.5	380.
	GTO	1.984	59.1	384.
$Ni_2, 2S_z = 2, *$	PMT	2.088	65.0	352.
	PMT(NR)	2.109	59.4	322.
	GTO	2.127	63.2	311.
$Cu_2, 2S_z = 0, *$	PMT	2.218	52.3	269.
	PMT(NR)	2.250	48.1	255.
	GTO	2.251	48.7	256.
$Zn_2, 2S_z = 0$	PMT	3.162	1.6	48.2
	PMT(NR)	3.167	2.0	51.8
	GTO	3.207	1.7	53.0
$Ga_2, 2S_z = 2$	PMT	2.725	35.7	152.
	PMT(NR)	2.732	36.4	153.
	GTO	2.738	36.1	155.
$Ge_2, 2S_z = 2$	PMT	2.414	72.4	273.
	PMT(NR)	2.420	73.3	275.
	GTO	2.423	72.6	272.
$As_2, 2S_z = 0$	PMT	2.112	96.5	433.
	PMT(NR)	2.119	97.8	434.
	GTO	2.125	96.8	434.
$Se_2, 2S_z = 2$	PMT	2.194	93.9	378.
	PMT(NR)	2.198	95.2	379.
	GTO	2.207	93.9	375.
$Br_2, 2S_z = 0$	PMT	2.309	57.3	314.
	PMT(NR)	2.311	58.1	315.
	GTO	2.328	54.6	305.
$Kr_2, 2S_z = 0$	PMT	4.334	0.154	14.7
	PMT(NR)	4.355	0.275	14.5
	GTO	4.413	0.191	16.3

problem solver for systems including both solids and molecules.

Acknowledgments

We thank Professor H. Akai for careful reading of and useful discussions on this manuscript. We appreciate our discussions with Professors T. Oguchi, S. Blügel, and P. Blöchl. This work was supported by a Grant-in-Aid for Scientific Research (23104510).

1) T. Kotani, M. van Schilfgaarde, and S. V. Faleev: Phys. Rev. B **76** (2007) 165106.
2) C. Friedrich, M. C. Müller, and S. Blügel: Phys. Rev. B **83** (2011) 081101.
3) R. Martin: *Electronic Structure: Basic Theory and Practical Methods* (Cambridge University Press, Cambridge, U.K., 2000).
4) P. E. Blöchl: Phys. Rev. B **50** (1994) 17953.
5) G. Kresse and D. Joubert: Phys. Rev. B **59** (1999) 1758.
6) D. J. Singh: *Planewaves, Pseudopotential, and the LAPW Method* (Kluwer Academic, Boston, MA, 1994).
7) S. Blügel and G. Bihlmayer: in *Computational Nanoscience: Do It Yourself!*, ed. D. M. J. Grotendorst and S. Blügel (John von Neumann Institute for Computing, Jülich, 2006) NIC Series, Vol. 31, pp. 85–129.
8) M. Methfessel, M. van Schilfgaarde, and R. A. Casali: *Lecture Notes in Physics*, ed. H. Dreysse (Springer, Berlin, 2000) Vol. 535.
9) O. K. Andersen: Phys. Rev. B **12** (1975) 3060.
10) J. M. Soler and A. R. Williams: Phys. Rev. B **47** (1993) 6784.
11) D. Singh: Phys. Rev. B **43** (1991) 6388.
12) K. Iwashita, T. Oguchi, and T. Jo: Phys. Rev. B **54** (1996) 1159.
13) M. Weinert, G. Schneider, R. Podloucky, and J. Redinger: J. Phys.: Condens. Matter **21** (2009) 084201.
14) T. Kotani and M. van Schilfgaarde: Phys. Rev. B **81** (2010) 125117.
15) J. P. Perdew, K. Burke, and M. Ernzerhof: Phys. Rev. Lett. **77** (1996) 3865.
16) J. A. White and D. M. Bird: Phys. Rev. B **50** (1994) 4954.
17) E. Bott, M. Methfessel, W. Krabs, and P. C. Schmidt: J. Math. Phys. **39** (1998) 3393.
18) E. Sjöstedt, L. Nordstrom, and D. J. Singh: Solid State Commun. **114** (2000) 15.
19) J. Paier, R. Hirschl, M. Marsman, and G. Kresse: J. Chem. Phys. **122** (2005) 234102.
20) A. J. Cohen, P. Mori-Sanchez, and W. Yang: Science **321** (2008) 792.